Tip-splitting evolution in the idealized Saffman–Taylor problem



2006 J. Phys. A: Math. Gen. 39 1759

(http://iopscience.iop.org/0305-4470/39/7/018)

INSTITUTE OF PHYSICS PUBLISHING JOURNAL OF PHYSICS A: MATHEMATICAL AND GENERAL

J. Phys. A: Math. Gen. **39** (2006) 1759–1765 doi:10.1088/0305-4470/39/7/018

# Tip-splitting evolution in the idealized Saffman–Taylor problem

**Eldad Bettelheim**[1] **and Oded Agam**[2]

[1] James Franck Institute, University of Chicago, 5640 S. Ellis Ave., Chicago, IL 60637
[2] Racah Institute of Physics, Hebrew University, Jerusalem 91904, Israel

E-mail: eldadb@phys.huji.ac.il

Received 17 November 2005, in final form 5 January 2006
Published 1 February 2006
Online at stacks.iop.org/JPhysA/39/1759

**Abstract**
We derive a formula describing the evolution of tip splittings of Saffman–Taylor fingers in a Hele–Shaw cell, at zero surface tension.

PACS numbers: 02.30.Ik, 05.45.Df, 05.45.Yv

Fingered patterns characterize the non-equilibrium growth processes of many systems, for example, the dendritic shape of snowflakes, the outline of bacteria colonies growing in stressed environments, electro-deposition, dielectric breakdown, and viscous fingering formed by forcing a non-viscous fluid into the centre of a Hele–Shaw cell filled with a viscous fluid (Saffman–Taylor flow) [1]. Repeated events of tip splittings and side branching during the growing process manifest themselves in complicated fractal patterns. Understanding the structure of such patterns is a challenge for theorists.

When the growing patterns are self-similar, one expects that their global structure can be deduced from the basic elements of the growing process, such as tip splitting and side branching. Indeed, studies of theoretical models of diffusion limited aggregation [2], and their generalizations (e.g. the dielectric breakdown model) demonstrate that the fractal dimension of the corresponding patterns is related to characteristics of the tip-splitting events [3] (side branching in these models is negligible).

In this work we focus our attention on the fingered patterns generated by Saffman–Taylor (ST) flows in a Hele–Shaw cell, in the radial geometry. In particular, we shall be interested in the evolution of tip splitting in the singular limit where the surface tension associated with the interface between the viscous and the non-viscous fluids approaches zero (or alternatively high pumping rate of the non-viscous fluid). The ST dynamics in this limit, which we shall refer to as the idealized ST problem, has been shown to be integrable [4]. Therefore, it constitutes an important paradigm in the field of non-equilibrium growth processes.

The idealized ST problem admits a large class of exact solutions [5–7]. Among these one may find solutions which resemble various forms of tips split at large surface tension [8]. These solutions are characterized by a smooth evolution of the bubble counter for any

  

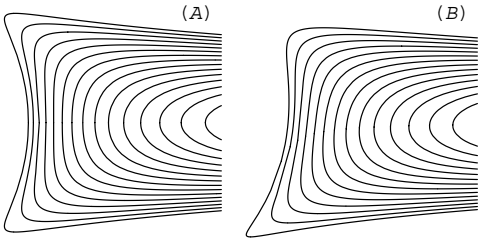


**Figure 1.** The evolution of tip splittings in the Saffman–Taylor problem at zero surface tension. The contours represent snapshots of the evolution as function of the time. The evolution given in (1) is characterized by one parameter, $\phi$, which controls the asymmetry between the two generated fingers. Panel A shows the symmetric evolution, while panel B represents a typical asymmetric behaviour.

time. Yet, these solutions lack universality since they depend on precise details of the initial conditions.

Nevertheless, there is another class of solutions of the idealized ST problem: solution which exhibit a cusp-like singularity after finite time. A generic ST bubble always develops a cusp. The cusp singularity dominates the evolution in its vicinity, and therefore it is expected to be universal. Thus, our aim is to describe the local dynamics near cusps of tip splitting.

Our central result is, thus, a formula which describes the evolution of tip splitting in time. It has the form

$$z(s,t) = s^2 + u_\phi(t) + \frac{v_\phi(t)}{w_\phi(t) + \mathrm{i}s}, \tag{1}$$

where $z = x + \mathrm{i}y$ is a complex coordinate on the bubble contour, $-\infty < s < \infty$ parametrize the curve, and $u_\phi(t)$, $v_\phi(t)$ and $w_\phi(t)$ are functions of the time, $t$. These functions which will be calculated in what follows, depend on a single parameter, $\phi$, governing the asymmetric shape of the evolution. In figure 1 we depict contours obtained from (1) which represent snapshots of the tip-splitting evolution as function of the time.

A problem one encounters when trying to describe the tip-splitting evolution is that a naive extension of the idealized ST dynamics beyond the cusp singularity is impossible. One may try to compute the ST dynamics, in the vicinity of a cusp, by introducing some infinitesimal surface tension. This approach indeed regularizes the problem but the resulting equations are nonintegrable, and the analytical treatment becomes very complicated [9]. There are some exact steady-state solutions, with surface tension, but these do not exhibit tip splitting [10].

Alternatively, the cusp singularity may be resolved by a method known as 'dispersive regularization' [11, 12], which preserves the integrable structure of the problem. This approach is similar, in spirit, to the construction of Gurevitch–Pitaevskii solutions for the KdV equation [13]. Its application to the ST problem is discussed extensively in[3]. Here we shall focus on time intervals where these aspects of the regularization are irrelevant.

We begin by recalling the ST problem. The local velocity of a viscous fluid in a thin cell is proportional to the gradient of the pressure $\vec{v} \propto \vec{\nabla} p$, where $p(z)$ is a harmonic function due to incompressibility. In the zero surface tension limit, the pressure may be taken to be equal to zero on the perimeter of the bubble, while at infinity it diverges logarithmically. At constant flow rate, the area of the bubble grows linearly with time, $t$. We set the flow rate such that the area is $\pi t$. The other parameters, viscosity and width of the cell, are chosen such that the pressure is equal to the velocity potential.

[3] E. Bettelheim *et al*, in preparation.

An important feature of the ST dynamics, at zero surface tension, is the conservation of the harmonic moments: $\frac{\mathrm{d}t_k}{\mathrm{d}t} = 0$, where

$$t_k = -\frac{1}{\pi k}\int_{\text{visc.fluid}} \mathrm{d}^2 z z^{-k}, \qquad k = 1, 2, \ldots. \tag{2}$$

and the integration is over the domain occupied by the viscous fluid. This property implies that the idealized ST dynamics is integrable, i.e. the bubble's contour can be determined from the set of harmonic moments, $t_k$'s, and the area $\pi t$. Our goal is to describe the evolution of this contour in the vicinity of the tip splitting.

In order to do so, it is instructive to introduce a potential defined as $V(z) = t\log(z) + \sum_k t_k z^k$. In particular, it will be convenient to work with sets of harmonic moments for which the potential can be resummed as

$$V(z) = t\log(z) + t_1 z + \sum_{i=1}^{N} \mu_i \log(z - q_i). \tag{3}$$

Thus, the set $\{t_k\}_{k=1}^{\infty}$ is replaced by a new set of parameters $\{\mu_i\}_{i=1}^{N}$ and $\{q_i\}_{i=1}^{N}$ known as Miwa variables in the soliton literature [14]. In particular $q_i$ and $\mu_i$ are, respectively, the location and the weight (assumed to be real) of the $i$th Miwa variable.

The potential defined above encodes the shape of the bubble in a rather complicated way. A function from which it is easier to extract this information is the Schwarz function. This function has proved to be a useful tool for the analysis of the ST problem (see e.g. [10, 15, 16]). A Schwarz function, $S(z)$, of a given contour $\mathcal{C}$ satisfies the relation $S(z) = \bar{z}$ (where $\bar{z}$ is the complex conjugate of $z$) for points $z$ which lie on the contour $\mathcal{C}$. Away from the contour it is defined via analytic continuation. The simplest example is a circular contour of area $\pi t$, whose Schwarz function can be easily deduced to be $S(z) = \frac{t}{z}$.

The Schwarz function is related to the set of harmonic moment by the contour integral $t_k = \frac{1}{2\pi \mathrm{i}}\oint_{\mathcal{C}} S(z) z^k \,\mathrm{d}z$. It implies that, on the exterior of the bubble, $S(z)$ has the same singular structure as $\frac{\partial V(z)}{\partial z}$ (as can be seen by deforming the contour integral such that it envelopes the singularities of $S(z)$ on the exterior of the bubble). Thus the analytic structure of $S(z)$ in the exterior domain, can be extracted from the potential, $V(z)$.

To reveal the analytic behaviour of $S(z)$ in the interior of the bubble one may employ an important property of the Schwarz function known as the unitarity condition,

$$\bar{S}(S(z)) = z, \tag{4}$$

where the complex conjugation of a function, $\bar{f}(z)$, is defined as $\overline{f}(z) \equiv \overline{f(\bar{z})}$. The equation above trivially holds for $z \in \mathcal{C}$ and by analytic continuation all over the complex plane. $S(z)$ maps points from the exterior of the bubble (where the analytic structure is known) to points on the interior domain. Thus all singularities of $S(z)$ can be identified, and hence its precise analytic form, as a function of the Miwa variables and the time.

We proceed by assuming that the Schwarz function is an algebraic function, i.e. a function defined on some algebraic Riemann surface. Let us explain what is an algebraic Riemann surface, and then describe how to define a Schwarz function on this surface. Consider a polynomial equation of the form $P(z, f(z)) = 0$, where $P$ is a polynomial in two variables. Solving this equation we obtain for each $z$ a set of solutions $f(z)$. In general $f(z)$ will have branch cuts. A simple example of such a polynomial is $P(z, f) = f^2 - \Pi_{i=1}^{4}(z - \lambda_i)$, where we obtain $f(z) = \sqrt{\Pi_{i=1}^{4}(z - \lambda_i)}$. In general there will be $n$ solutions of $f$ for each $z$. Thus one may introduce $n$ copies of the complex plane, where each copy is associated with a well-defined value of $f(z)$. Clearly, on each copy of the complex plane $f(z)$ is discontinuous along the branch cuts. To define it as a continuous function we may paste together the various

sheets of the complex plane along the branch cuts. Then, together with a choice of local coordinate systems around each point one obtains a Riemann surface composed of $n$ sheets.

Since we assume that the Schwarz function may be defined on such a Riemann surface, one should assign for each point on the Riemann surface, a value of Schwarz function, $S$. In order to specify such a point we must indicate the sheet-index $i$ (where $1 \leqslant i \leqslant n$), and a complex number $z$. The index, $i$, will specify on which copy of the complex plane the point lies, and a complex number, $z$, will specify the coordinate on that copy. There will be one copy of the complex plane, which will be termed as 'the physical sheet', on which the bubble lies. On this Riemann sheet $S(z)$ will be equal to $\bar{z}$ on the perimeter of the bubble. All other 'unphysical' Riemann sheets will be considered as parts of the 'interior domain' since there are no branch cuts on the exterior domain (where the pressure is harmonic).

Let us now consider a situation where the potential has the form (3), and show that the number of unphysical sheets is the number of Miwa variables. On the exterior of the bubble $S(z)$ has the following singular structure determined by $\frac{\partial V}{\partial z}$:

$$S(z) \sim \frac{t}{z} + t_1 - \sum_{i=1}^{N} \frac{\mu_i}{z - q_i}.$$

For the point $q_i$, unitarity (4) implies that $\bar{S}(S(q_i)) = \bar{S}(\infty) = q_i$. Thus a point at infinity should be mapped to the point $\bar{q}_i$. This point should be located on one of the unphysical sheets since on the physical sheet $S(\infty) = t_1$. Conversely, the value of the Schwarz function at infinity on an unphysical sheet correspond to a particular Miwa variable. From here on we consider the case of two Miwa variables, which is the minimal model exhibiting a tip-splitting scenario. The corresponding Riemann surface is thus composed of three sheets.

For actual calculation of the contour's evolution it will be convenient to use a conformal mapping which maps the exterior of some 'source domain' (in $\zeta$-plane) to the exterior of the physical bubble, the 'target domain' (in $z$-space). The source domain is usually taken to be the unit circle; however, we found it more convenient to use a bubble with a cusp. The advantage in using this source domain is that we can choose the mapping to be non-trivial only around the tip, while everywhere else it would be approximately proportional to the identity map.

We will study the evolution near the tip in the case where the weight of one of the Miwa variables is small compared to the other. This suggests choosing the source domain to be the one Miwa-variable bubble at the point where a cusp is formed. The Riemann surface in this case is composed of two sheets as described above. If we assume this surface to be of genus zero, then by the Riemann–Hurwitz theorem, the number of branch points is two. Thus the Riemann surface is given by the polynomial equation $R^2 = (\zeta - \lambda_1)(\zeta - \lambda_2)$. A function defined on this surface (the Schwarz function in particular) contains a branch cut which extends from point $\lambda_1$ to point $\lambda_2$. An example of such a function is $R(\zeta)$.

The 1-Miwa bubble is characterized by four parameters $t_1, t, q$ and $\mu$, since the location of the branch points depends on these parameters, one can calculate the area of the bubble and its first harmonic moment, $t_1$, from the location of the branch points $\lambda_1$ and $\lambda_2$. We will fix $\mu = -q = 1$ and treat $\lambda_1$ and $\lambda_2$ as the parameters which describe the bubble. If we also demand that the bubble is at the moment where the cusp forms, we can characterize the bubble by a single parameter, say $\lambda_1$. We assume that $\lambda_1 < \lambda_2$ and that $\lambda_1$ is of order $\delta$, where $\delta \ll 1$. This assumption implies that the global bubble shape is dominated by the cusp. Then the bubble area is of order $\delta^3$ while the first harmonic moment, $t_1$, is $1 + O(\delta^2)$. The Schwarz function, $\sigma(\zeta)$, of such a bubble is

$$2\sigma(\zeta) = (t_1 - 1) + \frac{t - 1}{\zeta - \bar{t}_1} - \frac{1}{\zeta + 1} + \frac{(t_1 + 1)(\zeta - \lambda_1)R(\zeta)}{(\zeta - t_1)(\zeta + 1)},$$

as can be ascertained by examining this function's singular structure and that it satisfies the unitarity condition (4). The fact that this function describes a bubble with a cusp can be checked by considering the behaviour of the solution of $\sigma(\zeta) = \bar{\zeta}$ near $\lambda_1$ (where the cusp is located).

Up till now we have characterized the 'source domain'. We would like, now, to specify the physical bubble, or the 'target domain' associated with two Miwa variables. For this purpose we must give the mapping between the source and target domains. This mapping is taken to be

$$z(\zeta) = c_1 \left( \zeta + \frac{\alpha}{2} \frac{R(\theta) - R(\zeta)}{\zeta - \theta} + \beta R(\zeta) \right) + c_2, \tag{5}$$

where $c_1$, $c_2$, $\alpha$, $\beta$ and $\theta$ are parameters of the mapping and $R(\zeta) \equiv \sqrt{\zeta - \lambda_1}\sqrt{\zeta - \lambda_2}$. This mapping can be considered as a mapping from the 1-Miwa Riemann surface to the 2-Miwa Riemann surface. The mapping has singularities at the infinities on each of the sheets of the Riemann surface associated with the source domain, which are mapped to infinites on different sheets on the target domain, as well as at the point $\theta$ on the unphysical sheet. This point, $\theta$, is mapped to an infinity on a third sheet of the target Riemann surface. Thus (5) indeed maps a two-sheeted Riemann surface, which is associated with a 1-Miwa bubble, to a three-sheeted Riemann surface.

That, indeed, the target Riemann surface is associated with a 2-Miwa variable bubble, can be deduced from the singular structure of the Schwarz function of the target domain. The latter is given by $S(z) = \bar{z}\,(\sigma\,(\zeta\,(z)))$, where $\zeta(z)$ is the inverse map of $z(\zeta)$, and $\sigma(\zeta)$ is the Schwarz function of the source domain.

Having $S(z)$ one may extract all constants of motion (Miwa variables, $q_1$, and $q_2$; Miwa weights, $\mu_1$ and $\mu_2$; and $t_1$), and the area $t$, from its singular structure. These will be expressed as functions of the parameters of the mapping (5) and $\lambda_1$. Solving these relations one may express the parameters of the mapping as functions of the time and thus obtain the evolution of the contour. We take $\mu_1 = -q_1 = 1$ by fixing $c_1$ and $c_2$. Thus the parameters whose time evolution is to be determined are $\alpha$, $\beta$, $\theta$ and $\lambda_1$.

To obtain reasonably simple equations, we expand all quantities in orders of $\delta$ and take the leading order. Let us assume that for some initial moment, $t^{(0)}$, around the formation of the tip, $\lambda_1$ assumes the value $\lambda$, to leading order in $\delta$. We now make the following scaling ansatz: $\alpha \sim \delta^4$, $\beta \sim \delta^3$, $\nu \equiv \lambda_1 - \theta \sim \delta^3$ and $\delta\lambda \equiv \lambda_1 - \lambda \sim \delta^3$. Then the equations we obtain, to leading order in $\delta$, for the constants of motion $q_2 - \lambda$ and $\mu_2$ are

$$q_2 - \lambda = \beta + \delta\lambda - \bar{\nu} - \frac{\alpha\sqrt{-\lambda}}{\sqrt{\nu} + \sqrt{\bar{\nu}}} \tag{6}$$

$$\mu_2 = -2\bar{\alpha}\sqrt{-\lambda}\sqrt{\nu}\left(1 - \frac{\alpha\sqrt{-\lambda}}{2\sqrt{\bar{\nu}}\left(\sqrt{\nu} + \sqrt{\bar{\nu}}\right)}\right). \tag{7}$$

Let us now define $T_1 = t_1 - \left(1 + 3\lambda^2 - 7\lambda^3 + \frac{33}{2}\lambda^4\right)$ (the difference between the first harmonic moment of the target bubble and a source bubble with $\lambda_1 = \lambda$ to order $O(\delta^5)$), and similarly $T = t - (-4\lambda^3 + 18\lambda^4 - 63\lambda^5)$. With these definitions, analysis of the singularities of $S(z)$ yields

$$T = 2\Re(\alpha)\lambda + 4\beta\lambda^2 - 12\lambda^2\delta\lambda, \tag{8}$$

$$T_1 = \Re(\alpha) - 2\beta\lambda + 6\lambda\delta\lambda. \tag{9}$$

The solution of equations (6)–(9) give the parameters $\alpha$, $\beta$, $\nu$ and $\delta\lambda$ in terms of $q_2$, $\mu_2$, $T$ and $T_1$, which define, in turn, the conformal mapping of the contour on the target space as function of the time. To write down the solution of these equations it will be convenient to define a shifted rescaled time $\delta t \equiv -\frac{T+2T_1\lambda}{4\mu_2^{3/4}\sqrt{-\lambda}}$ and introduce two functions $\xi$ and $\eta$ which satisfy the nonlinear equations:

$$\left(\frac{\sqrt{2}\delta t}{\sqrt{\xi}}+\frac{\delta t^2}{2\xi^2}\right)(\eta+\xi)=1, \qquad \eta=\left(\frac{\phi}{\sqrt{\xi}-\frac{\delta t}{\sqrt{2\xi}}}\right)^2,$$

where $\phi=\Im(\frac{q_2}{\sqrt{\mu_2}})$ is the asymmetry parameter. The solution of these equations gives $\eta$ and $\xi$ as functions of the rescaled time, $\delta t$, and $\phi$. With the help of these functions we may write the solution of equations (6-9) as

$$\begin{aligned}
\alpha &= \frac{\mu_2^{3/4}\delta t}{\sqrt{-\lambda}}\left(-1+\mathrm{i}\sqrt{\frac{\eta}{\xi}}\right),\\
4\beta &= 3\Re(q_2)-3\lambda-\frac{3}{2}(\eta-\xi)-\frac{3\delta t}{\sqrt{2\xi}}-\frac{T_1}{4\lambda}+\frac{T}{8\lambda^2},\\
\nu &= \frac{\xi-\eta}{2}+\mathrm{i}\sqrt{\xi\eta},\\
4\delta\lambda &= 3\Re(q_2)-3\lambda-\frac{3}{2}(\eta-\xi)-\frac{3\delta t}{\sqrt{2\xi}}+\frac{T_1}{4\lambda}-\frac{T}{8\lambda^2}.
\end{aligned}$$

Given this time dependence of the parameters of the conformal mapping we are in a position to describe the contour dynamics in the vicinity of the tip splitting. For this purpose it is sufficient to focus on the image of the source domain around the cusp. The shape of the source domain near the cusp is given by the universal form $y=A\delta x^{3/2}$, were $\delta x\equiv x-\lambda_1$, and $A$ is some constant. Close enough to the cusp $y\ll\delta x$, and therefore we may assume that $y\simeq 0$ (this assumption can be proved to be consistent with the expansion in the parameter $\delta$ performed above). Thus one has to find the image of the ray $x>\lambda_1$ under the mapping $z(\zeta)$ to leading order in $\delta$. The result is given by equation (1), where the functions $u_\phi(t)$, $v_\phi(t)$ and $w_\phi(t)$ are

$$\begin{aligned}
u_\phi(t) &= \frac{\xi-\eta}{2}-\frac{\delta t}{\sqrt{2\xi}},\\
v_\phi(t) &= \delta t\left(1-\mathrm{i}\sqrt{\frac{\eta}{\xi}}\right),\\
w_\phi(t) &= \frac{\xi-\eta}{2}+\mathrm{i}\sqrt{\eta\xi}.
\end{aligned}$$

The above equations together with (1) describe the evolution of a tip splitting of the ST problem at zero surface tension (figure 1). The form of the tip splitting depends on a single parameter, $\phi$, which controls the asymmetric shape of the evolution. Since our derivation of the tip-splitting formula makes use only of local properties near the tip, it is suggestive that this evolution, for short times, is universal. Namely, the tip-splitting evolution is characterized by one parameter, $\phi$, independent of the shape of the bubble on large scales. The shortcomings of our analysis is that it does not include the influence of surface tension. Therefore it breaks down after a short time due to the formation of cusps. The method of dispersive regularization can be employed again to continue the evolution. Thus, in comparing our theoretical prediction with experiment, one can hope for agreement only within a limited time interval near the initial stage of the tip splitting.

We thank Paul Wiegmann and Anton Zabrodin for useful discussions. This research has been supported in part by the Israel Science Foundation (ISF), and by the German-Israel Foundation (GIF).

## References


[1] Halsey T C 2000 *Phys. Today* **53** 36
[2] Witten T A and Sander L M 1983 *Phys. Rev.* B **27** 5686
[3] Halsey T C and Leibig M 1992 *Phys. Rev.* A **46** 7793
[4] Mineev-Weinstein M, Wiegmann P B and Zabrodin A 2000 *Phys. Rev. Lett.* **84** 5106 (*Preprint* nlin.si/0001007)
[5] Howison S D 1986 *J. Fluid Mech.* **167** 439
[6] Bensimon D, Kadanoff L P, Liang S D, Shraiman B I and Tang C 1986 *Rev. Mod. Phys.* **58** 977
[7] Richardson S 1972 *J. Fluid Mech.* **56** 609
[8] Hohlov Y E and Howison S D 1993 *Q. Appl. Math.* **51** 777
[9] Siegel M, Tanveer S and Dai W 1996 *J. Fluid Mech.* **323** 201
[10] Vasconcelos G L 1993 *Phys. Rev.* E **48** 658
[11] Whitham G B 1966 *SIAM J. Appl. Math.* **14** 956
[12] Bloch A M and Kodama Y 1992 *SIAM J. Appl. Math.* **52** 909
[13] Guervich A V and Pitaevski L P 1974 *Sov. Phys.—JETP* **38** 291
[14] Jimbo M and Miwa T 1983 *Publ. RIMS Kyoto Univ.* **19** 943
[15] Cummings L J, Howison S D and King J R 1999 *Eur. J. Appl. Math.* **10** 635
[16] Davis P J 1974 The Schwartz function and its applications (USA: The Mathematical Association of America)